

# Water Immersion Optical Lithography for the 45nm Node

Bruce W. Smith, Hoyoung Kang, Anatoly Bourov, Frank Cropanese, Yongfa Fan  
Rochester Institute of Technology, Microelectronic Engineering Department  
82 Lomb Memorial Drive, Rochester, NY 14623

## ABSTRACT

It is possible to extend optical lithography by using immersion imaging methods. Historically, the application of immersion optics to microlithography has not been seriously pursued because of the alternative solutions available. As the challenges of shorter wavelength become increasingly difficult, immersion imaging becomes more feasible. We present results from research into 193nm excimer laser immersion lithography at extreme propagation angles (such as those produces with strong OAI and PSM). This is being carried out in a fluid that is most compatible in a manufacturable process, namely water. By designing a system around the optical properties of water, we are able to image with wavelengths down to 193nm. Measured absorption is below  $0.50 \text{ cm}^{-1}$  at 185nm and below  $0.05 \text{ cm}^{-1}$  at 193nm. Furthermore, through the development of oblique angle imaging, numerical apertures approaching 1.0 in air and 1.44 in water are feasible. The refractive index of water at 193nm (1.44) allows for exploration of the following:

1.  $k_1$  values approaching 0.17 and optical lithography approaching 35nm.
2. Polarization effects at oblique angles (extreme NA).
3. Immersion and photoresist interactions with polarization.
4. Immersion fluid composition, temperature, flow, and micro-bubble influence on optical properties (index, absorption, aberration, birefringence).
5. Mechanical requirements for imaging, scanning, and wafer transport in a water media.
6. Synthesizing conventional projection imaging via interferometric imaging.

**Keywords:** Optical lithography, immersion, excimer laser, optical extension

## 1. INTRODUCTION

Optical lithography has been driven toward sub-100nm dimensions using means now considered “conventional”. High NA, phase-shift masking, modified illumination, optical proximity correction, and pupil filtering are being employed. Fabrication challenges have been aggressively pursued so that 65m device geometry may be possible using wavelengths as large as 193nm. Lithography at 157nm is positioned for 45-65 nm technology, extending optical methods yet further along the semiconductor technology roadmap. Though the shorter wavelength of 157nm is beneficial, additional resolution enhancement is needed to ensure that this technology is viable or is multi-generational. The problems with such a short wavelength have introduced associated risks.

As an alternative, we have also started exploring methods to allow longer UV wavelength imaging technology for application to sub-70nm device nodes. Though the 193nm ArF wavelength may be feasible for 70nm lithography, conventional imaging would not allow resolution beyond this. There is merit in the exploration into optical lithography methods that will make use of the resolution potential of extreme-NA immersion imaging, where the numerical aperture of the imaging tool approaches the immersion media index. If numerical aperture (NA) values above 1.0 were possible via immersion, sub-quarter wavelength lithography could be obtained (note that numerical aperture is defined for the purpose of this description as the *sin* of the half acceptance angle,  $q$ ). This represents a departure from conventional thinking where gains have been paralleled with source wavelength reduction.

Ernst Abbe was the first to discover that the maximum ray slope entering a lens from an axial point on an object could be increased by a factor equal to the refractive index of the imaging media [1]. He first realized this in the late 1870's by observing an increase in the ray slope in the Canada balsam mounting compound used in microscope objectives at the time. To achieve a practical system employing this effect, he replaced the air layer between a microscope objective and a cover glass with oil having a refractive index in the visible near that of the glass on either side. This index matching prevents reflective effects at the interfaces (and total internal reflection at large angles),

leading to the term “homogenous immersion” for the system he developed. The most significant application of the immersion lens was in the field of medical research, where oil immersion objectives with a high resolving power were introduced by Carl Zeiss in the 1880’s. Abbe and Zeiss developed oil immersion systems by using oils that matched the refractive index of glass. This has resulted in numerical aperture values up to a maximum of 1.4 allowing light microscopes to resolve two points distanced only 0.2 microns apart (corresponding to a  $k_1$  factor value in lithography of 0.5).

An important requirement needed to benefit from the potential of immersion imaging is an objective lens specifically designed for this application. Ray angles (and the corresponding numerical aperture) cannot be increased by merely placing an immersion fluid between an objective lens and the image plane. Furthermore, the spherical aberration induced through this increase in refractive index can be substantial and will lead to image degradation. Imaging through an immersion media represents a parallel plate situation. By applying aberration theory of two interfaces, imaging and aberration results can be evaluated [2]. The wavefront aberration function through the two interfaces of the media can be written as:

$$W(\rho, \theta; h) = \alpha(\rho^4 - 4h\rho^3\cos(\theta) + 4h^2\rho^2\cos^2\theta + 2h^2\rho^2 - 4h^3\rho\cos\theta)$$

Where  $h$  is the separation of an object point from the optical axis,  $\alpha$  is the weighted aberration coefficient, and  $\rho$  is the normalized radius of the pupil. The five terms of the function describe spherical, coma, astigmatism, defocus, and tilt respectively. The aberration coefficient  $a$  in an immersion distance is:

$$\alpha = \frac{t(n^2 - 1)}{8n^3S^4}$$

where  $t$  is the thickness of the fluid,  $n$  is refractive index and  $S$  is the separation distance from the lens pupil.

An objective lens would be specifically designed for this application to allow for larger ray angles and for the interfacing of these angles with the immersion fluid. The most frequently used form of an immersion lens includes a hemispherical element in optical contact with the fluid. Figure 1 shows methods that could be used to interface an optical system with an immersion fluid. In each case, the left most component represents an optical element (a flat plate, a prism, or a hemispherical lens), the center component is the immersion fluid, and the right most component is the photoresist detector. The flat plate element allows for interfacing of an optical system but does not offer any advantage through an increase in ray angle. The prism and hemispherical elements allow for an increase in ray angle via the coupling of the ray in air at normal incidence. The numerical aperture in the resist remains constant ( $n_{pr}\sin q_{pr}$ ). This NA is preserved through the immersion fluid and through the optical element by Snell’s law. The advantage of these two approaches is realized when one considers the numerical aperture that would have been needed in air to produce the resulting NA values in the immersion fluid and in the photoresist. There is an increase in the effective NA in the air proportional to the refractive index of the immersion fluid (assuming that the optical element is index matched to this fluid).

The advantages of immersion lithography may be better represented through an effective scaling of wavelength rather than numerical aperture. This is a consequence of the impact that imaging into an immersion media has on focal depth. The substitution of an immersion effective NA value into the Rayleigh DOF relationship suggests an improvement with  $n^2$ . This is an incorrect description since focus scales linearly with  $n$ . A more appropriate equation for immersion DOF is given as:

$$DOF = \pm k_2 \lambda_i / \sin^2 q$$

where  $\lambda_i$  is the wavelength in the imaging media rather than vacuum [3]. Figure 2 shows how the wavelength of a wavefront is reduced from  $\lambda_0$ , its value in vacuum (air), to  $\lambda_i$ . The effective wavelength in water at 193nm becomes 193/1.44 or 134nm.

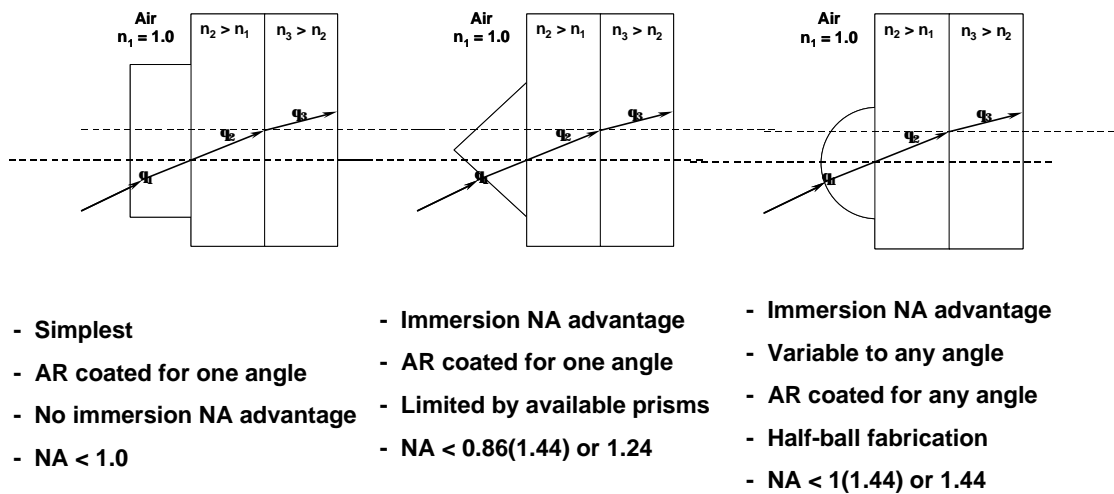


Figure 1. Optical interfacing with an immersion fluid.

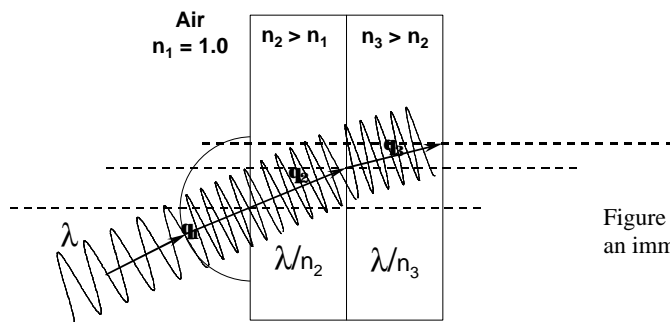


Figure 2. Refractive effects reducing the effective wavelength in an immersion media..

The choice of immersion fluids is based primarily on their transparency, where many additional challenges remain in order to benefit from their imaging potential. As wavelengths are increased from the VUV, liquids with more attractive properties have sufficient transmission for use as immersion imaging fluids. The prime example is water, with absorption below  $0.50 \text{ cm}^{-1}$  at 185nm and below  $0.05 \text{ cm}^{-1}$  at 193nm. The refractive index of water at 193nm is 1.44, which would effectively decrease wavelength to 134nm *or* effectively increase the numerical aperture of an imaging system to 1.44 NA. The resolution is proportionally increased by the refractive index value. This represents a 43% potential improvement in resolution, which is twice that achieved with the wavelength transitions from 248nm to 193nm, from 193nm to 157nm, or from 157nm to 126nm. As a numerical aperture of 1.44 is approached, resolution to 35nm is theoretically possible using water immersion. Furthermore, there is a 17% potential resolution improvement using water immersion at 193nm when compared to 157nm conventional imaging for identical air-NA values. DOF for immersion imaging is calculated based on the effective reduction in wavelength, or  $\lambda/(nNA^2)$ . This is significant as the usable focal depth scales linearly with the media index rather than quadratically with the media NA. Water immersion lithography has potential to reduce the critical technical barriers and risks associated with driving optical lithography toward sub-50nm resolution. Technical challenges related to the development of the support technologies for water immersion lithography are also reduced compared to those for the potential immersion fluids for shorter wavelengths. Compatibility with scanning, purging, environment, resist and processes, in-situ metrology, cleaning, and thermal stability are examples. Furthermore, it is feasible to accomplish this at established wavelengths where other materials concerns (such as optical material absorption, expansion, and birefringence) are sufficiently low.

The exploration of the full potential and feasibility of water immersion lithography requires the development of extremely high NA (or extreme NA) imaging capability. This implies optical systems that would operate near an

equivalent air-media NA of 1.0, which is a difficult task in its own right. This situation can be addressed through the development of large angle interferometric imaging for 35-50nm patterning. As is the case with current trends in high NA projection lithography, the issues involved with imaging at such oblique propagation angles become significant. Though interferometric imaging has been carried out for many applications, such studies have concentrated on the ultimate imaging potential of interferometric lithography (IL), pushing half-pitch resolution to  $\lambda/(2\sin \theta)$ . Though these concepts may have promise, this is not the intent of the present research. Instead, interferometric imaging provides the opportunity to explore extreme NA imaging issues. There is much unknown regarding lithographic imaging using mostly oblique angles. This represents current and future optical lithography situations where diffraction energy in the lens pupil is limited such that images are created with the most extreme angles allowed.

## **2. IMMERSION LITHOGRAPHY AT 193NM**

Untapped lithography potential exists at UV/VUV optical wavelengths. This potential is more significant than the generational improvements in wavelength alone. The investigation into the resolution possible at current lithography wavelengths is being carried out through the exploration of immersion imaging at extreme propagation angles. By designing an immersion system around the optical properties of water, we are able to image at 193nm/1.44 (or effectively 134nm). Furthermore, through the development of interferometric imaging, numerical apertures approaching 1.0 in air and 1.44 in water are feasible. The refractive index of water at 193nm will allow for research into the following:

1. k1 values approaching 0.17 and optical lithography approaching 35nm.
2. Polarization effects at oblique angles (extreme NA).
3. Immersion and photoresist interactions with polarization.
4. Immersion fluid composition, temperature, and flow influence on optical properties (index, absorption, aberration).
5. Mechanical requirements for imaging, scanning, and wafer transport in a water media.
6. Synthesizing conventional projection imaging via interferometric

## **3. IMMERSION IMAGING SYSTEMS**

Immersion lithography has been explored in the past [4, 5] with little success for several reasons including:

1. UV resists release a significant volume of dissociated nitrogen through photochemical reaction upon exposure.
2. The relatively high index fluids at UV wavelengths tend to react with photoresist materials.
3. Standard immersion fluids are not transparent below 300nm.
4. Wafer handling processes of fluid wetting, cleaning, and drying add significant cost and complexity.
5. Alternative optical solutions existed.

Furthermore, the refractive index of water at UV wavelengths is not sufficiently high (~1.30) to warrant its use so that the above concerns (specifically numbers 1 through 3) could be alleviated.

The current situation for DUV/VUV lithography is quite different. Optical lithography is approaching the limits of wavelength, resolution, and conventional numerical aperture. Exploration into imaging methods that were previously considered impractical have become reasonable. The use of water as an immersion fluid is now an attractive choice for several reasons that are contrary to the problems in the past, including:

1. 193nm resist platforms release low volumes of gas during exposure.
2. The reaction of water with 193nm photoresist is minimal and can be reduced through modification of resist materials.
3. Water is transparent to below  $0.05 \text{ cm}^{-1}$  at 193nm.
4. Water is an existing component of wafer processing, limiting the critical concerns of wetting, cleaning and drying.
5. Few alternative optical choices now exist.

#### 4. WATER IMMERSION LITHOGRAPHY CHALLENGES

One goal of the current research is to explore and understand the issues involved with water immersion imaging at 193nm. Additionally, prototype systems are being built for the project in order to measure the important parameters associated with immersion lithography. Several critical issues exist, which are being addressed in order to develop the technology required for commercialization of immersion lithography in water. A fundamental issue is the compatibility of water with conventional lithography components. The technical risks associated with water immersion imaging are reduced when compared to some fluids but they require exploration. Water can be easily purified, limiting adverse optical effects. The interaction with conventional resist platforms can be made minimal through proper solvent and process choices.

Extensive data exists regarding the static optical properties of water. The application of immersion lithography will most likely be in a scanning mode in order to maximize the optical field and pupil capabilities. An understanding of the index, birefringence absorption and dispersion of immersion fluids under pressure and flow are critical for this application. Measurements are being carried out by fabricating a conventional (Michelson) interferometer to measure path length variation (OPD) in a calcium fluoride cell containing the immersion fluid temperature controlled within  $0.1^\circ\text{C}$ . Index, absorption, and dispersion measurements are being carried out as fluid temperature, flow, and pressure are varied. This data will provide the foundation for the specification of imaging and scanning requirements.

Substrate handling, fluid introduction, fluid removal, scanning, and other interfacing support technologies need to be proven feasible to establish the proposed technology as viable. One area that needs to be explored is the dynamics of the spreading properties of water when it is used in a scanning immersion system. The behavior of the immersion fluid depends on the interactions of the fluid with the solid surfaces of the resist/wafer substrate and the final optical element. The current models for the behavior of wetting and spreading of fluids require exploration. Research conducted in this area will lead to the understanding of the dynamics involved. The optical effects of dissolved gases in water will be studied. The influence of pressure, flow, temperature, and surface conditions will be explored and required solutions will be developed.

Several optical challenges exist for the development of an immersion imaging technology. The variations of the refractive index of fluids with temperature, pressure, and wavelength are included in these challenges. Index variation with wavelength (or dispersion,  $dn/d\lambda$ ) can result in a chromatic aberration effect where acceptable limits can be determined through analysis. For example, if a fluid working distance of a few millimeters is considered, the color dispersion in this region should be sufficiently smaller than optical depth of focus. For the paraxial case, the optical path length of the fluid with is simply the product of the refractive index ( $n$ ) and the fluid thickness ( $t$ ). For a high NA case, the optical path difference should be less than  $\lambda/4$  and  $dn$  should be no greater than:

$$dn = \frac{\lambda \cos \theta}{4t}$$

which leads to the definition of the control requirements for the factors influencing index including wavelength, temperature, pressure, etc. Table 1 shows the extent of index change (in ppm) for path lengths of 1, 5, and 10mm using this equation.

Working Distance (mm)	NA					
	0.7	0.8	0.9	1	1.1	1.2
10	4	4	4	4	3	3
5	8	8	8	7	6	6
1	42	40	38	35	32	28

Table 1. Index control requirement for an immersion fluid at 193 nm in ppm .

With regard to index variation with temperature ( $dn/dT$ ), our measurements show that the refractive index of water changes about  $150 \text{ ppm } ^\circ\text{C}^{-1}$  (using interferometric measurement techniques at UV and visible wavelengths). Based on this data and the results in Table 1, it is reasonable to assume that temperature control to  $0.1 \text{ }^\circ\text{C}$  is adequate for NA values of 1.0 and above with sufficient working distances.

Our recent data on the absorption and the temperature dispersion properties are shown in Figures 3 and 4. This data is further encouragement that the technical challenges associated with water immersion lithography at 193nm are surmountable.

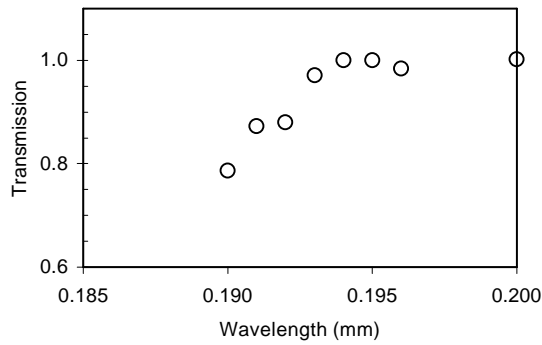


Figure 3. Transmission properties of 1cm of water near 193nm.

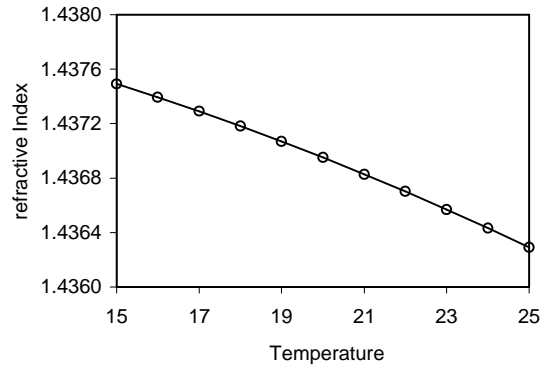


Figure 4. Temperature dispersion ( $dn/dT$ ) of water .

Additional process issues need exploration for the implementation of immersion imaging to lithography. Water can be easily made free of optical impurities. Interaction with conventional resist platforms can be made minimal through proper solvent and process choices. Several issues need to be addressed with regard to the introduction and flow of an immersion fluid. Although these concerns are common to many fluids, there are potentially fewer issues involved with the use of water. Concerns particular to water include:

1. An air curtain system may be a potential source of trapped air into the water layer. A possible solution will be to devise a surface tension driven water retaining structure.
2. The release of gas at the resist/wafer surface may be problematic. Gas may also be released with the VUV radiation used for resist exposure. If this is an issue, then the water stream velocity needs to be maintained such that gas is absorbed readily without causing microbubble formation.

3. Microbubble formation may occur on the cavities present at the resist/wafer surface. As water moves over these cavities during optical system traverse, a certain amount of air is trapped in the cavities. UV exposure energy incident on the submerged surface may also encourage bubble growth.
4. The water itself should be free of microbubbles. The use degassed water may be required. This could be a non-existent problem if the gas release does not occur with incident radiation.
5. Surface wetting and dewetting characteristics are important aspects. Chemical control of these parameters is possible.

## 5. INTERFEROMETRIC IMAGING AT 193NM

Interferometric lithography provides an opportunity to explore lithographic imaging at oblique propagation angles and extreme NA imaging. Through interferometric imaging, a sinusoidal standing wave pattern is created through the interference of coherent wavefronts. Through the control of the number of wavefronts and their corresponding interference angle, the orientation, pitch and dimensionality of geometry can be controlled. By including a non-interfering component, imaging can be tailored to synthesize various conventional projection imaging situations. Through variation of the phase character of a plurality of wavefronts, imaging can be matched to those obtained using partially coherent projection lithography. The advantage of using IL as a method to achieve such images is the versatility to allow for high NA values and immersion imaging media.

Interferometric lithography at 193nm has historically been difficult because of the poor temporal and spatial coherence characteristics of the excimer laser. Interferometric lithography at 157nm is assisted by the nature of the emission of the F<sub>2</sub> laser. Various achromatic schemes have been introduced for ArF excimer lasers [6] but are not practical for this application due to the constraints of the configuration for one single imaging condition. We have explored the feasibility of modifying the operation a ArF 193nm excimer to the specifications required for this application. Extra-cavity spatial and temporal filtering can allow for output of a modified 100 Hz 4W commercial compact excimer laser (GAM EX10) to operate to the following specifications:

Energy Control Range mJ 4-12  
Repetition Rate 100 Hz  
Pulse Length 15 nS  
Beam Size 8 X 3-5 mm, Divergence 1 X 2 mRad  
Stability <2% Standard Deviation  
Temporal coherence 0.5mm (optional to 1 -2 mm)  
Spatial Coherence >0.5mm  
Beam Uniformity +/-5%

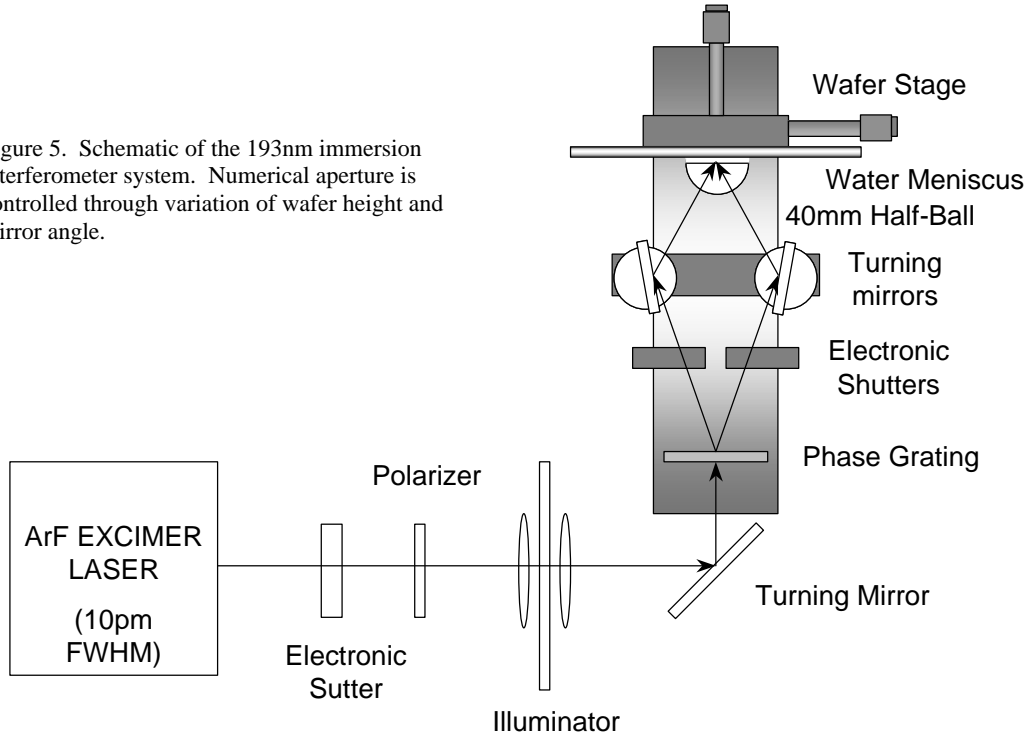
By expanding the beam to 10 cm, we allow for the following operation:

Pulse energy 5mJ  
Dose per pulse ~0.1mj/cm<sup>2</sup>  
Spatial coherence region 5mm  
Field uniformity 1% in 2mm

The effect of the spatial coherence and spectral width can be correlated to the useful field size for an imaging IL system based on this 193nm source, leading to the following parameters:

Critical path length control ~ 0.35mm  
Beam misalignment requirement 0.8mm  
Usable field size for 90% contrast 2mm

Figure 5. Schematic of the 193nm immersion interferometer system. Numerical aperture is controlled through variation of wafer height and mirror angle.



The application of a Talbot interferometer has been used for excimer laser interferometric imaging [7]. The approach that we have taken is a variation on such a system where first order beams are split using a phase grating and recombined using a pair of mirrors to form an interference pattern. The setup is shown in Figure 5. In a system with  $d/2$  reduction (where  $d$  is the grating pitch on the phase mask), the approach leads to an achromatic system when angles at the grating and image planes are equivalent. This is a consequence of the preservation of path length and spatial coherence within the beams. In the present system, a grating pitch of 550nm is used, resulting in a numerical aperture (NA) on the mask side of 0.18. We are interested in NA values close to 1.0 (and pitch values in air near 100nm or in water near 70nm). This requires that we vary the mirror and image plane angles to increase the image NA by a factor of 5. The achromatic behavior is therefore reduced and the dependence on spatial coherence is increased. The consequence is a reduction in usable field size and depth of focus, measure for example through a loss of image contrast. For a source with a spectral bandwidth  $\mathbf{Dl}$  over a phase range  $\mathbf{Df}$ , the angular misalignment can be calculated as:

$$DlDf < \frac{l_c d \cos^2 q_c \sin q_c}{(a + b)}$$

where  $a$  and  $b$  are the path lengths of the interferometer arms. The interference modulation for a pitch  $\Lambda$  can be calculated as:

$$I_{wafer}(x) = \text{Re} \left( \int E_{src}(\mathbf{l}) e^{i \frac{2\pi}{\Lambda(I)} x} d\mathbf{l} \right)^2$$

Techniques exist to utilize interferometric lithography to synthesize the functions of conventional projection photolithography. The method employed with this system involves the intensity attenuation of one of the first diffraction orders being interfered. A portion of the remaining beam is not interfered when the intensity of the first beam is reduced. This results in a background energy equivalent to the zero order. The interferometric lithography system can be altered to produce varying duty ratios by manipulating the level of the zero order intensity through the attenuation of a single beam. The waveform with lower zero order amplitude bears a smaller space width and a larger line width than the waveform with a larger zero order bias. The ability to synthesize the function of projection lithography comes with a tradeoff in the loss of contrast for duty ratios deviating from 1:1. The loss in contrast occurs due to increase in background energy from the zero order bias. Examples of transmission - duty ratio correlation are listed in Table 2.

Duty Ratio l:s	Pitch	0 <sup>th</sup>	1 <sup>st</sup>	Trans.
1:0.4	1.4	0.286	0.249	0.50
1:1	2	0.500	0.318	0.40
1:2	2.9	0.655	0.281	0.30
1:2.65	3.65	0.726	0.241	0.25
1:3.7	4.7	0.787	0.197	0.20

Table 2. Duty ratios synthesized using interferometric imaging and single beam attenuation.

## 6. POLARIZATION EFFECTS AT EXTREME NA

Non-scalar imaging effects result as the propagation angles of the electric field for extreme-NA imaging become large. At oblique angles, radiation polarized in the plane of incidence exhibits reduced image contrast. This polarization state is referred to as *TM* or *p* polarization with respect to vertically oriented geometry. As angles approach  $\pi/4$  [or  $\sin^{-1}(1/\sqrt{2})$ ], no interference exists in air and image contrast is reduced to zero. For polarization perpendicular to the plane of incidence (*TE* or *s* polarization), complete interference exists and no reduction in image contrast will result. For non-linear polarization, an image is formed as the sum of *TE* and *TM* image states.

Very low  $k_1$  imaging with extreme-NA will result in the most oblique image propagation angles. There are significant differences in the *TE* and *TM* aerial image polarization states at these extreme angles. When an image exists in a high index media, *TM* polarization contrast loss is governed by the limiting angle which is increased by the media index ( $n$ ) as  $\sin^{-1}(n/\sqrt{2})$ . With immersion imaging, the fluid index is not the determinant for this limiting angle, however, as the image is ultimately directed into a photoresist material. Furthermore, the separation of polarization components via reflection at media interfaces is reduced as index matching is possible with the absence of air in the optical path. This is a significant advantage introduced with immersion lithography as the coupling of the preferred *TE* polarization state is usually reduced as an image is translated from air media to photoresist. For a 193nm resist material at an air NA value of 0.95, as much as 40% of the *TE* image state is reduced at the air/resist interface, resulting in contrast loss in the absence of a large angle, strong anti-reflective layer. When utilized in a water immersion mode, more than 95% of the *TE* image state is coupled into the resist film.

Though polarization and high NA lithography effects have been addressed for some time, an understanding of these effects for oblique angle imaging at extreme NA values does not exist. Interdependencies of resist index, media index, absorption, diffusion, interfacial, and thin film aberration effects need to be fully explored. Figure 6 shows the calculated *TE* vs. *TE* modulation for imaging in air and in water when the numerical aperture for the water case is scaled for the water index. The simulations were made by normalizing the wavelength, resist, and substrate index values to the refractive index of water to model the effects of changing the imaging media from the air assumption of the simulator (Proith/7 vector model). The prediction was confirmed with experimentation using the 457 nm line of the Ar ion laser was used as the light source, providing excellent temporal and spatial coherence for this setup. A  $\lambda/4$  plate combined with a linear polarizer was used to alter the polarization state of the source, rotating it by  $\pi/2$ . The mirror angle was adjusted so that different arrival angles ( $\theta$ ) could be achieved. The contrast of the image was calculated by measuring the dose to appear ( $E_a$ ) and the dose to disappear ( $E_d$ ) of the resist images. The image contrast was thus calculated using

$$C = \frac{E_d - E_a}{E_d + E_a}$$

The metric of interest for this study represents the degradation of contrast when source polarization is changed from TE to TM. Simple calculations show that the ratio of TM to TE image contrast should be constant for both dry and immersed setups. Results are shown in Figure 7.

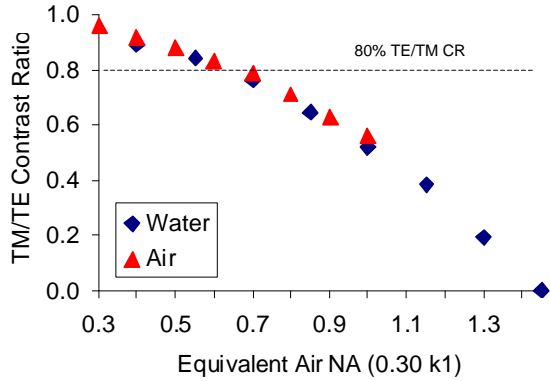


Figure 6. TM vs. TE polarization contrast from simulation.

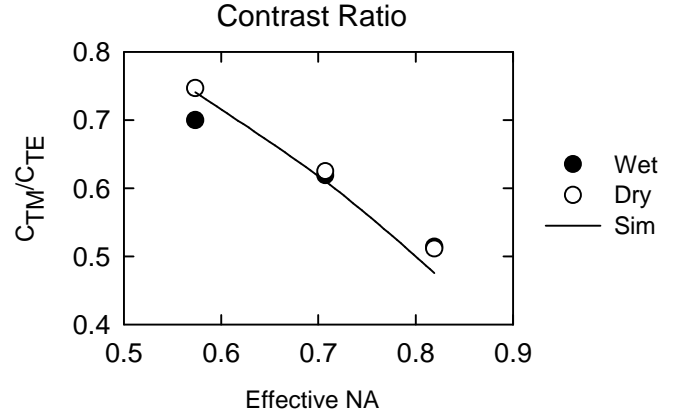
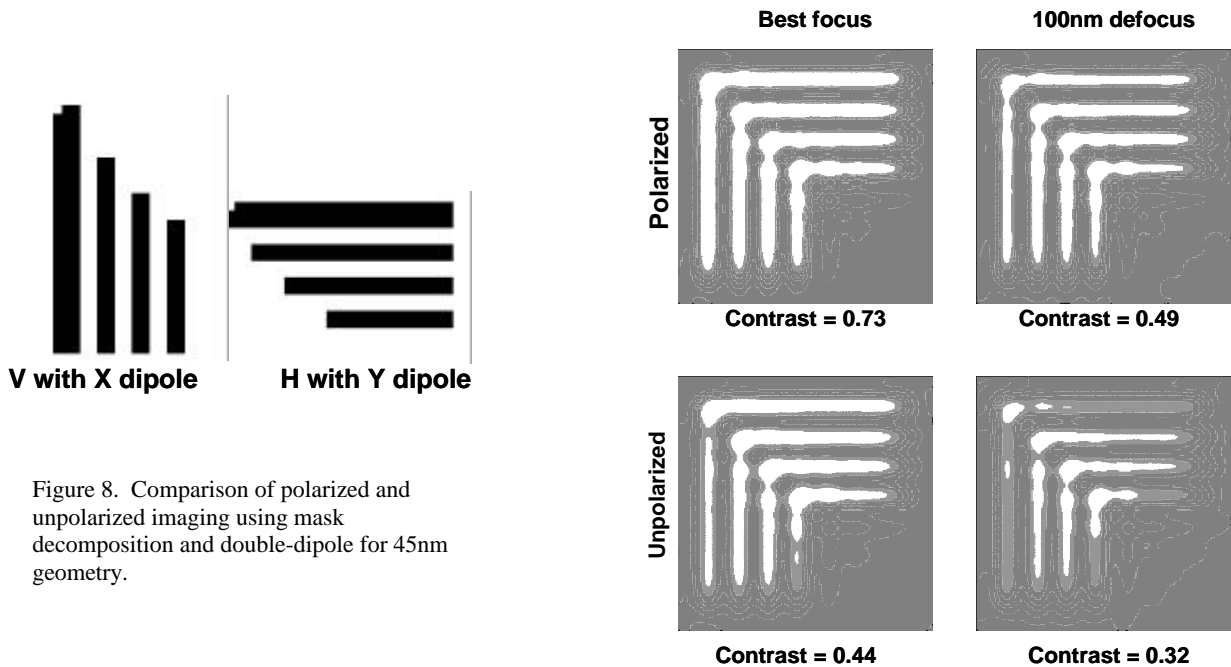


Figure 7. Experimental comparison of air and water imaging.

## 7. DECOMPOSITION OF IMAGING FOR EXTREME NA AND POLARIZATION

As we move into the regime of extreme NA with approaches that include immersion imaging, methods must be explored that will take full advantage of the potential. Figure 8 shows a simulated example of imaging 45nm X-Y geometry by decomposing the mask into horizontal and vertical components and imaging with dipole illumination. A comparison is shown of the impact of using TE polarized imaging vs. unpolarized imaging. An increase in image modulation is obtainable with polarized illumination, especially when defocus is considered. Imaging to sub-0.3 k<sub>1</sub> is only likely for such large NA values only when polarization methods are also employed.



## 9. CONCLUSIONS

This work describes the feasibility of immersion lithography for application to imaging below 65nm. The use of water at 193nm is attractive over other fluids at shorter wavelengths because of the transmission and refractive index properties of water at this wavelength. Several issues are being addressed to explore the feasibility of the technology for application to device manufacturing. These include imaging capability, fluids properties (including bubbles), and resist interactions. These are currently under exploration.

## 10. REFERENCES

1. E. Abbe, 1878.
2. V. Mahajan, *Aberration Theory Made Simple*, SPIE Press, Vol. TT (1991) 30.
3. B.J. Lin, "The  $k_3$  Coefficient in Nonparaxial  $\lambda/NA$  Scaling Equations for Resolution, Depth of Focus, and Immersion Lithography," *JM<sup>3</sup>* 1(1), 7, 2002.
4. US 4,480,910.
5. US 4,509,852.
6. T. Savas et al, *J. Vac. Sci. Technol. B* 13(6), 2732, 1995
7. P.E. Dyer, R.J. Farley, R. Giedl, *Opt. Comm*, 129, 98, 1996.

- 
1. E. Abbe, 1878.
  2. V. Mahajan, Aberration Theory Made Simple, SPIE Press, Vol . TT (1991) 30.
  3. B.J. Lin, "The  $k_3$  Coefficient in Nonparaxial  $\lambda/NA$  Scaling Equations for Resolution, Depth of Focus, and Immersion Lithography," *JM<sup>3</sup>* 1(1), 7, 2002.
  4. US 4,480,910.
  5. US 4,509,852.
  6. T. Savas et al, *J. Vac. Sci. Technol. B* 13(6) 1995, 2732
  7. P.E. Dyer, R.J. Farley, R. Giedl, *Opt. Comm*, 129, 1996, 98.